

Lattice dynamics of ionic FeBr₂

G. Benedek and I. Pollini

Istituto di Fisica dell'Università di Milano and Gruppo Nazionale di Struttura della Materia del Consiglio Nazionale delle Ricerche, Via Celoria 16, 20133 Milano, Italy

(Received 25 March 1982)

Yelon *et al.* shell-model analysis of neutron scattering data on FeBr₂ leads to the conclusion that the crystal has a very small ionicity. We have reexamined their neutron data on the ground of our previous extended-shell-model theory and infrared measurements, which are here supplemented by new data on high-concentration samples. Our analysis confirms the high ionicity of this crystal, and the fitting procedure provides information on the static dipole and anisotropy of the effective charges.

This Brief Report follows the work by Benedek and Frey on the lattice dynamics of transition-metal dihalides based on the extended-shell model (ESM) (Ref. 1) and the optical studies on the same materials reported by Pollini *et al.*² The subsequent neutron scattering measurements of the phonon dispersion curves in FeBr₂ by Yelon *et al.*³ have stimulated the present work. These authors have performed also a theoretical fit of their neutron data by means of the static-displaced-shell model (SDSM) already used by Pasternak in the analysis of FeCl₂ and CoCl₂.^{4,5} Unfortunately, the information on the electrical constitution of FeBr₂ coming from such SDSM calculation is rather unphysical. In particular, the ionicity is found to be exceedingly low ($Z = 0.162e$), in contrast with the highly ionic character of these compounds emerging from the large LO-TO splittings,^{6,7} the crystal-field spectra,² and the measurements of transferred hyperfine field⁸; moreover, the static dipole W_0Y at the halide ion is about three times small-

er than the value derived from electrostatics.¹ On the other hand, the neutron data of Yelon *et al.* appear to reproduce adequately the earlier ESM calculation (Fig. 1). This calculation was based exclusively on thermochemical, Raman,⁹ and infrared data,² with a net charge of $Z = 0.83e$, an isotropic Szigeti charge of $Z^s = 0.572e$, and $W_0Y = 0.40 \text{ \AA}$, which are in the appropriate physical range. Therefore it seemed to us worthwhile discussing the neutron data on FeBr₂ in the light of ESM calculation, in order to get reliable knowledge on the effective charges and static dipoles.

We see in Fig. 1 that the original ESM calculation follows quite well the measured dispersion curves. In particular, the flat dispersion of the optical branches along the c axis and the upper acoustic branches in all directions are well reproduced. There is some disagreement concerning the lower TA branch along Σ and T and the optical branch ending at E_u^L along Σ . These discrepancies, however, are quite interesting since they can be removed through a fine adjustment

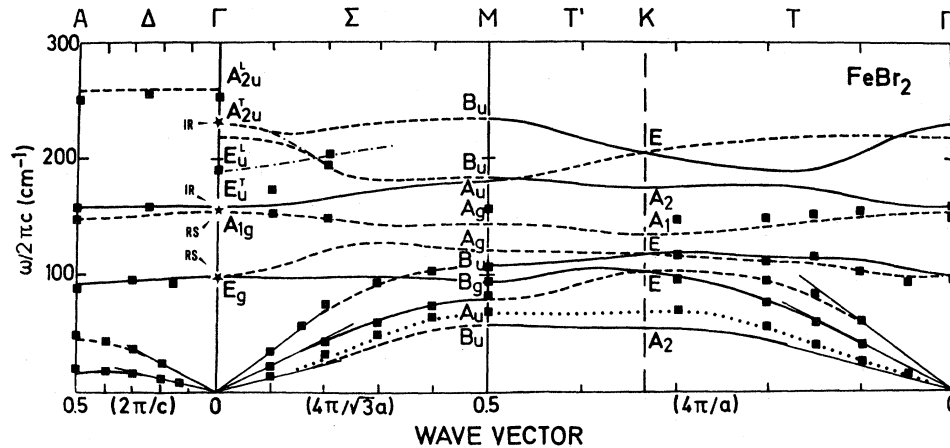


FIG. 1. Dispersion curves of FeBr₂(C₆) obtained by ESM calculation. Dashed (full) lines correspond to $A_1(E)$, $A'(A'')$, and $A(B)$ modes along Δ , Σ , and T directions, respectively (from Ref. 1). Dotted line: See text. Stars indicate experimental Raman and infrared frequencies (Refs. 2 and 7). Black squares are the phonon modes measured by inelastic neutron scattering.

of our relevant parameters: the static dipole and the anisotropy of effective charges.

As shown in Figs. 13–16 of Ref. 1 the lowest acoustic modes at M and K (B_u and A_2 , respectively) are extremely sensitive to the Coulomb field of the static dipoles. If a static dipole moment $W_0Y = 0.46 \text{ \AA} e$ is used instead of $0.40 \text{ \AA} e$, the discrepancy in the lower TA branch is completely removed (dotted line) without sensible effects on the other phonon branches all over the Brillouin zone. Moreover, this value of W_0Y is closer to the electrostatic value $\mu_0^{(1)} = 0.51 \text{ \AA} e$ calculated for the undistorted lattice configuration (the so-called first-iteration value¹).

In order to discuss the situation occurring in the optical branches at point Γ , we have tried to improve the precision of infrared absorption measurements. The present far-infrared (FIR) absorption spectra were recorded at room temperature on powder samples dispersed in polyethylene, which was chosen as a supporting medium because it has a good transparency in the range $40\text{--}400 \text{ cm}^{-1}$. Samples were prepared by mixing tiny crystals freshly grown from the vapor phase with polyethylene in a dry atmosphere. The mixture was heated in a mold to melt the polyethylene in order to form on cooling a disk of about 5 cm in diameter. With these precautions the samples should be almost free from contamination of atmospheric moisture. Second-order infrared spectra were observed on specimens in which the sample concentration was high enough to show saturation in the one-phonon absorption region.

The neutron experimental frequency $\omega_T = 187 \text{ cm}^{-1}$ at the zone center is here assigned to E_u^L (instead of A_{2u}^T as in Ref. 3) since no structure is observed in the far-infrared absorption spectrum at that value [Fig. 2(a)]. The lowest significant bump in FIR spectrum which can be associated to A_{2u}^T occurs at $226 \pm 4 \text{ cm}^{-1}$. The ESM calculations were based on this assignment, which, on the other hand, scales well with the other bromides of the family.² Moreover, the spectrum taken from a high-concentration sample [Fig. 2(b)] shows possible combination bands of the assigned E_u^T and A_{2u}^T frequencies with the frequencies of A_{1g} and E_g Raman-active modes. In Fig. 2(b) we have marked also the crystal-field transitions $(1, \pm 1) \rightarrow (2, 0)$, $(2, \pm 1)$, $(2, \pm 2)$ within Fe^{2+} ground state ${}^5T_{2g}(D)$ as known from Raman spectroscopy above

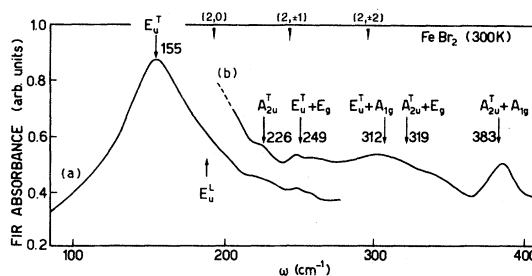


FIG. 2. Room-temperature far-infrared absorption of powdered FeBr_2 in polyethylene matrix. Powder samples of low (a) and high (b) concentrations were considered. Arrows indicate active infrared A_{2u}^T and E_u^T modes and their combination bands with A_{1g} and E_g Raman active modes and crystal-field transitions within the ${}^5T_{2g}(D)$ ground state of the d^5 configuration (from Ref. 10).

T_N (Ref. 10) $(2, \pm 1)$ and $(2, \pm 2)$ are slightly below the second-order structures involving E_u^T , so that the attributions of the latter could be questionable, while no electronic transition corresponds to either A_{2u}^L or $A_{2u}^T + A_{1g}$. Still, the calculated E_u^L frequency is about 30 cm^{-1} above the experimental value. The larger LO-TO splitting for the E_u modes reflects the appreciable anisotropy of the calculated effective charges ($Z_{xx}^{\text{eff}} = 1.093e$, $Z_{zz}^{\text{eff}} = 0.854$, from Table V of Ref. 1) which are, in turn, rather sensitive on the few input data used in ESM calculations.

For an isotropic effective charge $Z_{xx}^{\text{eff}} = Z_{zz}^{\text{eff}} = 0.854$, the E_u LO-TO splitting is reduced in such a way that the disagreement between calculated and experimental E_u modes disappears. Actually, the two parallel branches $E_u^T - A_u$ and $E_u^L - B_u$ get closer, which could also yield a better fit of the highest point at $K = 0.2(4\pi/\sqrt{3}\bar{a})$ along Σ (dot-dash guideline).

In conclusion, the original ESM calculations of phonon dispersion curves in $3d$ metal dihalides have received further support from the neutron data on FeBr_2 , and this is implicitly true for the scale of ionicity and the corresponding values of the cohesive energy previously given^{1,2} for this class of solid compounds. In particular, the fine adjustment to neutron data yields a fitted anion dipole value closer to the electrostatic result and a smaller anisotropy of the transverse effective charges.

¹G. Benedek and A. Frey, Phys. Rev. B **21**, 2482 (1980).

²I. Pollini, G. Spinolo, and G. Benedek, Phys. Rev. B **22**, 6369 (1980).

³W. B. Yelon, C. Vettier, A. Pasternak, and H. Guggenheim, J. Phys. C **13**, 5863 (1980).

⁴A. Pasternak, J. Phys. C **9**, 2987 (1976).

⁵A. Pasternak, Solid State Commun. **26**, 685 (1978).

⁶B. Szigeti, Trans. Faraday Soc. **45**, 155 (1949); Proc. R. Soc. London Ser. A **204**, 51 (1950).

⁷H. J. L. van der Valk and C. Haas, Phys. Status Solidi (b) **80**, 321 (1977).

⁸S. R. Kuindersma, C. Haas, J. P. Sanchez, and R. Al, Solid State Commun. **30**, 403 (1979).

⁹I. W. Johnstone, D. J. Lockwood, and G. Mischler, J. Phys. C **11**, 2147 (1978); G. Benedek, I. Pollini, L. Piseri, and R. Tubino, Phys. Rev. B **20**, 4303 (1979).

¹⁰I. W. Johnstone, D. J. Lockwood, and G. Mischler, J. Phys. C **11**, 2147 (1978).